A Leaky-Wave Analysis of the High-Gain Printed Antenna Configuration

DAVID R. JACKSON, MEMBER, IEEE, AND ARTHUR A. OLINER, LIFE FELLOW, IEEE

Abstract—**A leaky-wave analysis is used to explain the narrow-beam "resonance gain" phenomenon, in which narrow beams may be produced from a printed antenna element in a substrate-superstrate geometry. The leaky-wave approach furnishes insight into the physical processes involved, provides new practical information, and permits the derivation of simple asymptotic formulas for the leaky-wave properties and for the radiation behavior. Results are presented as a function of frequency, the scan angle, and the ϵ of the superstrate.**

I. Introduction

RECENTLY, a method for increasing the gain of a printed-circuit antenna involving the use of a superstrate layer was discussed [1]. In this method the antenna element is embedded within a two-layered geometry consisting of a bottom (substrate) layer of thickness b having relative permittivity and permeability ϵ_1, μ_1, and a top (superstrate) layer having parameters ϵ_2, μ_2, as shown in Fig. 1. As explained in [1], a narrow beam about any desired angle θ_p may be obtained for $\epsilon_2 \gg 1$ or $\mu_2 \gg 1$ when the layer thicknesses are chosen properly. In particular, the following dual types of "resonance conditions" are discussed in [1].

Case 1:

$$\frac{n_1 b}{\lambda_0}\sqrt{1-\sin^2\theta_p/n_1^2}=\frac{m}{2} \tag{1}$$

$$\frac{n_2 t}{\lambda_0}\sqrt{1-\sin^2\theta_p/n_2^2}=\frac{(2p-1)}{4} \tag{2}$$

for $\epsilon_2 \gg 1$.

Case 2:

$$\frac{n_1 b}{\lambda_0}\sqrt{1-\sin^2\theta_p/n_1^2}=\frac{(2m-1)}{4} \tag{3}$$

$$\frac{n_2 t}{\lambda_0}\sqrt{1-\sin^2\theta_p/n_2^2}=\frac{(2p-1)}{4} \tag{4}$$

for $\mu_2 \gg 1$, where $n_1 = \sqrt{\epsilon_1\mu_1}$, $n_2 = \sqrt{\epsilon_2\mu_2}$ and m, n are positive integers.

When (1), (2) or (3), (4) are satisfied, the gain at θ_p becomes increasingly large as $\epsilon_2 \to \infty$ or $\mu_2 \to \infty$, respectively, with a resultant decrease in beamwidth. Asymptotic formulas for gain and beamwidth are presented in [1]. Although providing for convenient formulas, this derivation does not by itself provide any *insight* into the fundamental cause of the narrow-beam phenomenon.

Manuscript received March 20, 1987; revised September 24, 1987. This work was supported in part by the Army Research Office under Contract DAAG29-84-K-0166.

D. R. Jackson is with the Cullen College of Engineering, University of Houston, 4800 Calhoun Road, Houston, TX 77004.

A. A. Oliner is with the Polytechnic University, 333 Jay Street, Brooklyn, NY 11201.

IEEE Log Number 8820226.

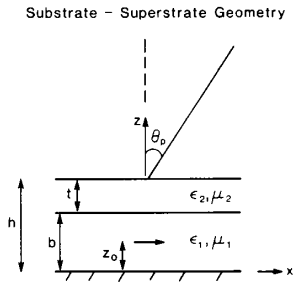

Fig. 1. Two-layered geometry with embedded dipole antenna element from which narrow beam can be radiated. ϵ_2 (or μ_2) of superstrate (upper layer) must be greater than ϵ_1 (or μ_1) of substrate. Horizontal antenna element is located at height z_0 and peak of radiated beam occurs at angle θ_p.

In this article it is shown that the resonance gain effect may be elegantly described in terms of *leaky waves*. It is demonstrated that the phenomenon is attributable to the presence of both transverse electric (TE)- and transverse magnetic (TM)-mode leaky waves which are excited on the structure. Asymptotic formulas for the leaky-wave properties are derived, which demonstrate that the attenuation rate of the leaky waves decreases as the gain of the pattern increases. The migration with frequency of the leaky-wave poles in the steepest-descent plane is also discussed, and it is shown that several important physical effects are confirmed by that investigation. Radiation patterns based on the relevant leaky wave are then compared with the exact patterns to demonstrate the dominant role of the leaky waves in determining the pattern. One practical result of this investigation is a simple rule for determining the size of the structure necessary to produce the narrow-beam patterns, a result which would be difficult to obtain otherwise.

Due to the similarity of results, only case 1 ($\epsilon_2 \gg 1$) will be discussed. This is the more practical of the two cases, since low-loss high-permeability materials are difficult to obtain.

II. Leaky-Wave Poles and the Steepest-Descent Representation

The theory of leaky waves and their role in determining the radiation behavior of certain antennas is well established [2]–[7]. To emphasize the main points, the analysis for the case of a horizontal Hertzian electric dipole in the stratified medium

0018-926X/88/0700-0905$01.00

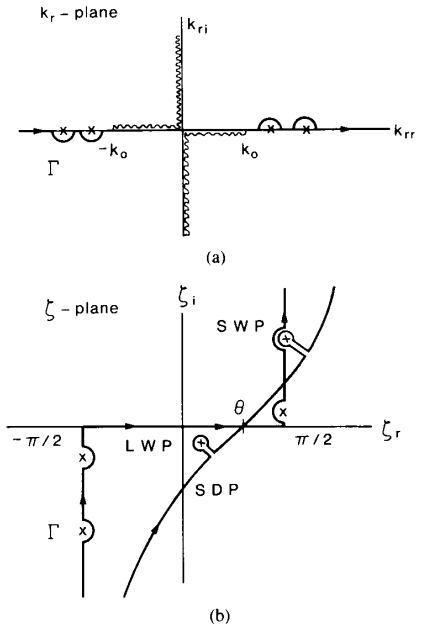

Fig. 2. (a) k_r-plane, where k_r is wavenumber transverse to z direction. Surface-wave poles lie along real axis (denoted by x's) and branch cuts (wiggly lines) emanate from branch points $\pm k_0$. Integration path Γ is deformed around surface-wave poles in accordance with conventional assumption of infinitesimal loss (and $e^{j\omega t}$ time dependence). Branch cuts are chosen so that upper Riemann sheet is proper, whereas lower Riemann sheet is improper. Leaky-wave poles occur on improper (lower) sheet. (b) Steepest-descent plane corresponding to time dependence $e^{j\omega t}$. Saddle-point is present at $\zeta = 0$ on real axis, and example is given of leaky-wave pole and surface-wave pole captured by deformation from original path Γ to steepest-descent path.

of Fig. 1 will be considered. Starting with the classical Sommerfeld solution [8], the expressions for the fields are written in terms of the Hertzian magnetic vector potential $\bar{\Pi}$ as

$$\bar{H} = j\omega\epsilon\nabla\times\bar{\Pi} \tag{5}$$

$$\bar{E} = k^2\bar{\Pi} + \nabla(\nabla\cdot\bar{\Pi}). \tag{6}$$

After solving the boundary-value problem for $\bar{\Pi}$, the two components of the potential Π_x and Π_z may be written in the region $z > h$ as (suppressing $e^{+j\omega t}$)

$$\Pi_x(r, z) = \int_{-\infty}^{+\infty} \frac{f(k_r r)}{D_e(k_r)} e^{-jk_z(z-h)} H_0^{(2)}(k_r r)\, dk_r \tag{7}$$

$$\Pi_z(r, z) = \cos\phi \int_{-\infty}^{+\infty} \frac{g(k_r r)}{D_e(k_r) D_m(k_r)} e^{-jk_z(z-h)} H_1^{(2)}(k_r r)\, dk_r \tag{8}$$

where

$$r = \sqrt{x^2 + y^2}$$

$$k_z = (k_0^2 - k_r^2)^{1/2}.$$

In these expressions f, g, D_e, and D_m are complicated functions [9] of the integration variable k_r. D_e and D_m have zeros on the real axis of the k_r plane in the range $k_0 \le k_r \le \max(k_i)$, where k_i is the wavenumber in the ith layer. These zeros correspond to TE- and TM-mode surface waves, respectively. The integration path goes around these poles, as shown in Fig. 2(a). Branch cuts from the branch points at $\pm k_0$ are also necessary to define the proper branch interpretation of k_z, which is Im $(k_z) < 0$, corresponding to fields that decay as z increases.

The steepest-descent transformation

$$k_r = k_0 \sin\zeta \tag{9}$$

$$k_z = k_0 \cos\zeta \tag{10}$$

then results in an integration along the contour Γ in the steepest-descent ζ-plane, shown in Fig. 2(b). This contour may be deformed into the steepest-descent path (SDP) which passes through the saddle point at $\zeta = \theta$, where R, θ, ϕ describe the observation point in spherical coordinates with $r = R\sin\theta$, $z - h = R\cos\theta$. The far-field evaluations of (7), (8) may be obtained via the saddle point method in the usual way [7]. It is important to recognize that the single-sheeted steepest-descent plane as a whole is neither proper nor improper, but in fact portions of it are proper and other portions improper. The semi-infinite strip for which $0 < \zeta_r < \pi/2$ and $\zeta_i < 0$ is an improper region (Im $(k_z) > 0$). Complex zeros of $D_e(k_r)$, $D_m(k_r)$ may exist in this region at $\zeta_{rp} + j\zeta_{ip}$, which result in TE- and TM-mode "leaky-wave" poles (LWP). Complex poles can only occur in the improper region for the lossless case when $\epsilon_i > 1$, $\mu_i > 1$ [2]. Hence the only other poles in the ζ-plane are the surface wave poles (SWP), which lie along the lines $\zeta_r = \pm\pi/2$, as shown.

If θ is sufficiently large, some leaky-wave poles will in general be captured during the path deformation, as shown in Fig. 2(b). The leaky-wave fields increase exponentially with z, but decrease exponentially with R within the region in which they are defined, since $\theta > \zeta_{rp}$ when they are captured [2]. The leaky-wave phase and attenuation constants are given by

$$\beta = \text{Re}\,(k_{rp}) = \text{Re}\,(k_0 \sin\zeta_p) = k_0 \sin\zeta_{rp}\cosh\zeta_{ip} \tag{11}$$

$$\alpha = -\text{Im}\,(k_{rp}) = -\text{Im}\,(k_0\sin\zeta_p) = -k_0\cos\zeta_{rp}\sinh\zeta_{ip}, \tag{12}$$

respectively, where $\beta - j\alpha$ is the pole location in the k_r-plane (on the improper sheet). If a leaky-wave pole is close to the real axis so that α is sufficiently small, the leaky-wave field will dominate the total field at the air-dielectric interface, provided the residue is not too small [3]. In this case the radiation pattern exhibits a sharply peaked behavior at $\theta = \theta_p$ where

$$\beta \simeq k_0 \sin\theta_p. \tag{13}$$

A more detailed discussion of leaky-wave properties is given in [2], [3].

III. Asymptotic Evaluation of the Leaky-Wave Properties

In view of the previous discussion, it may be expected that leaky waves could be responsible for the high-gain effect. This

presumption may be verified by a straightforward, but lengthy, asymptotic solution for the leaky-wave pole locations of the characteristic equations, which are as follows.

TE-Mode:

$$D_e = 0 = \cos(k_{z2}t)[\mu_1(jk_{z0}b) + (k_{z1}b)\cot(k_{z1}b)] - \frac{\sin(k_{z2}t)}{k_{z2}t}\left[\frac{\mu_1}{\mu_2}(k_{z2}t)(k_{z2}b) - j\mu_2(k_{z1}b)(k_{z0}t)\cot(k_{z1}b)\right]. \quad (14)$$

TM-Mode:

$$D_m = 0 = \cos(k_{z2}t)[j(k_{z0}b)\epsilon_1 - (k_{z1}b)\tan(k_{z1}b)] - \frac{\sin(k_{z2}t)}{k_{z2}t}\left[\frac{\epsilon_1}{\epsilon_2}(k_{z2}t)(k_{z2}b) + j\epsilon_2(k_{z1}b)(k_{z0}t)\tan(k_{z1}b)\right] \quad (15)$$

where

$$k_{z0} = (k_0^2 - k_r^2)^{1/2}$$
$$k_{z1} = (k_1^2 - k_r^2)^{1/2}$$
$$k_{z2} = (k_2^2 - k_r^2)^{1/2}.$$

The sign taken for the square root of k_{z1}, k_{z2} is arbitrary since these signs occur in even function fashion in (14) and (15), but Im $(k_{z0}) > 0$ is used to ensure the improper pole interpretation.

To solve for complex pole locations asymptotically, k_r is written as a perturbation about the expected high-gain value as

$$k_r = k_0 \sin\theta_p + k_0(\delta_r + j\delta_i). \quad (16)$$

The arguments of the tan and cot functions may then be approximated for the cases $\theta_p > 0$ and $\theta_p = 0$ and then substituted into (14), (15), with only the dominant terms kept as $\epsilon_2 \to \infty$. After straightforward but lengthy simplification, the results summarized below are obtained.

TE-Mode:

$\theta_p > 0$:

$$\beta/k_0 \sim \sin\theta_p \quad (17a)$$

$$\alpha/k_0 \sim a_1/\epsilon_2. \quad (17b)$$

$\theta_p = 0$:

$$\beta/k_0 \sim \alpha/k_0 \sim c_1/\sqrt{\epsilon_2}. \quad (17c)$$

TM-Mode:

$\theta_p > 0$:

$$\beta/k_0 \sim \sin\theta_p \quad (18a)$$

$$\alpha/k_0 \sim b_1/\epsilon_2. \quad (18b)$$

$\theta_p = 0$:

$$\beta/k_0 \sim \alpha/k_0 \sim c_1/\sqrt{\epsilon_2} \quad (18c)$$

where

$$a_1 = \frac{1}{m\pi}\frac{\mu_2}{\mu_1}(n_1^2 - \sin^2\theta_p)^{3/2}\cot\theta_p \quad (19a)$$

$$b_1 = \frac{1}{m\pi}\epsilon_1\mu_2(n_1^2 - \sin^2\theta_p)^{1/2}(\sin\theta_p\cos\theta_p)^{-1} \quad (19b)$$

$$c_1 = \frac{1}{\sqrt{m\pi}}\sqrt{\mu_2/\mu_1}\, n_1^{3/2}. \quad (19c)$$

Several important conclusions follow from these results. First, there exists a TE-mode and a TM-mode leaky-wave pole which both become dominant ($\alpha \to 0$) for $\epsilon_2 \gg 1$. For these dominant poles $\beta/k_0 \sim \sin\theta_p$ when $\theta_p > 0$, in agreement with the conclusion of a peaked beam at θ_p due to the leaky waves. For $\theta_p > 0$ the attenuation constant α behaves as $O(1/\epsilon_2)$. For the case $\theta_p = 0$, β/k_0 tends to zero, but relatively slowly, behaving as $O(1/\sqrt{\epsilon_2})$. In this case, α/k_0 has the same asymptotic form as β/k_0, and hence the leaky-wave pole asymptotically approaches the origin along the diagonal line, in either the k_r-plane or the ζ-plane. Furthermore, in this case the form is the same for both the TE- and TM-mode poles.

To verify the validity of the asymptotic formulas, results showing a comparison of the exact and asymptotic leaky-wave propagation wavenumbers for the TE-mode case are presented in Fig. 3 for a broadside beam, and in Fig. 4 for a scanned beam ($\theta_p = 45°$), for the lowest mode ($m = 1$, $p = 1$). The exact values are found by a secant-method search in the complex plane. The agreement is good in all cases, and improves as ϵ_r increases.

One of the *practical uses* of these formulas for the leaky-wave properties is in determining the required structure size in the x, y directions to realize the narrow beam patterns. The size required is such that the leaky waves emanating from the dipole are sufficiently attenuated at the perimeter. If the structure radius is r_s, then $\alpha r_s \gg 1$ is required.

IV. Leaky-Wave Radiation Patterns

The TE-mode leaky wave primarily determines the E_ϕ component of the far field, while the TM-mode wave primarily determines E_θ. The TM-mode leaky wave thus determines beamwidth in the E-plane, while the TE-mode wave determines beamwidth in the H-plane. Because the asymptotic form for α/k_0 is the same for the TE- and TM-modes when $\theta_p = 0$, a broadside pencil beam is produced which is circular in shape. For a scanned beam the forms are different, so a conical beam having different beamwidths in the two planes is created.

For the H-plane, it is possible to predict easily the leaky-wave radiation pattern using scalar diffraction theory. This is because the H-plane pattern of the dipole is the same as that for an infinite line source in the x direction. Because of the two-dimensional nature of the line-source problem, a scalar Kirchhoff–Huygens formulation may be used to determine the radiation field from the amplitude distribution of the leaky-wave on the layer surface. Derived in [3], the formula for the

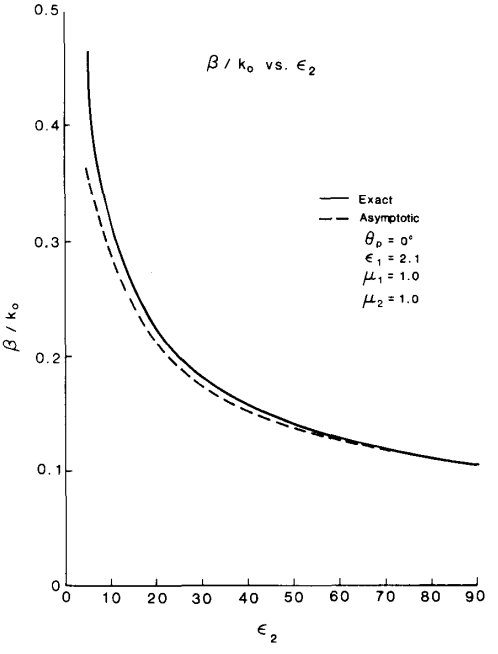

Fig. 3. Comparisons between exact and asymptotic TE-mode leaky-wave propagation wavenumbers as function of dielectric constant ϵ_2 of superstrate, for lowest mode with $\theta_p = 0°$ (broadside beam). (a) Phase constant β/k_0 versus ϵ_2. (b) Attenuation constant α/k_0 versus ϵ_2.

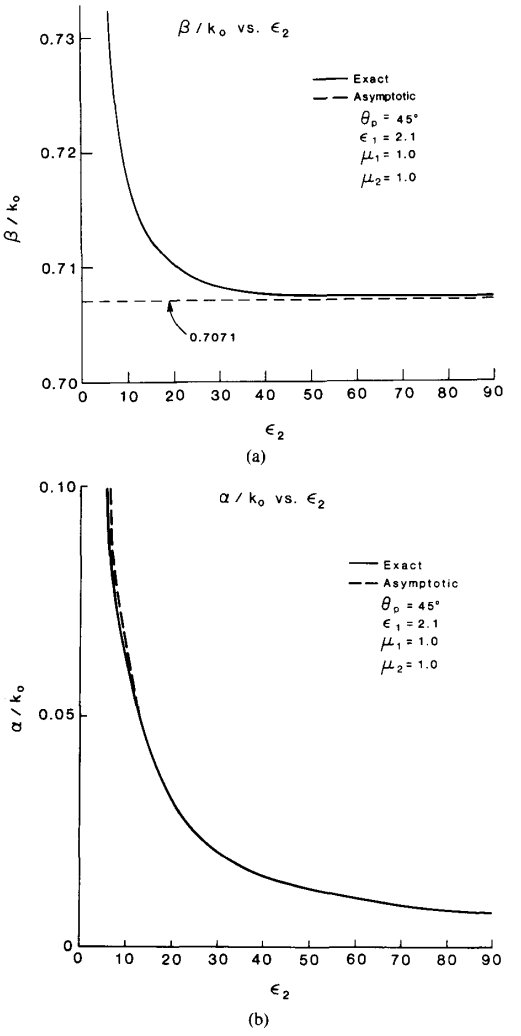

Fig. 4. Same as Fig. 3, but for $\theta_p = 45°$ (scanned beam). Note that in Fig. 4(a), for β/k_0, ordinate scale is greatly enlarged.

radiated power pattern is

$$R(\theta) = \left| \frac{\cos\theta}{\sin^2\zeta_p - \sin^2\theta} \right|^2. \tag{20}$$

To provide a convincing demonstration of the dominant nature of the leaky waves in determining the pattern, the exact H-plane radiation pattern (from a reciprocity method [1]) is compared with (20) for the lowest mode ($m = p = 1$) in Fig. 5(a) and (b) for $\theta_p = 0°$ and $\theta_p = 45°$, respectively (the patterns are normalized to 1.0 at the maximum). The agreement is excellent in both cases.

Since the asymptotic formulas for α/k_0 do not depend on the dipole position z_0 but only on the layer parameters, the beamwidth and gain of the pattern are likewise independent of z_0 in the asymptotic limit. The amount of radiated power is, however, dependent on the dipole position. The optimum

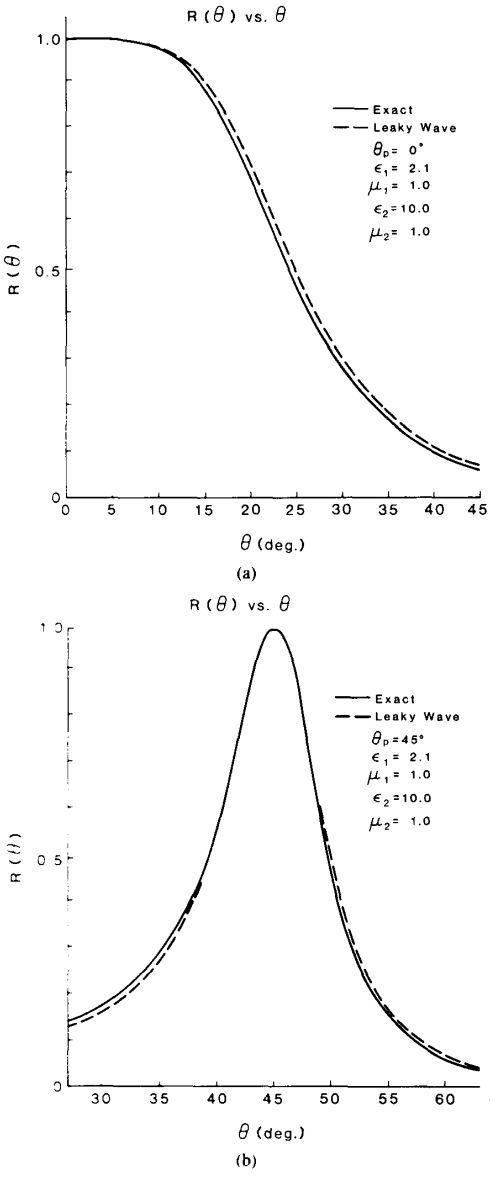

Fig. 5. Comparisons of exact and leaky-wave H-plane radiation patterns for lowest mode with $\epsilon_2 = 10$. (a) $\theta_p = 0°$. (b) $\theta_p = 45°$. Agreements are seen to be excellent.

dipole height to maximize radiated power is

$$\frac{n_1 z_0}{\lambda_0} \sqrt{1-\sin^2\theta_p/n_1^2} = \frac{1}{4}(2n-1), \qquad n=1, 2, \cdots \quad (21)$$

where $z_0 < b$. This places z_0 at a voltage maximum position in a transmission-line model of the layered structure [1].

V. Pole Migration With Frequency

Some interesting features can be observed as the leaky-wave pole positions are traced as a function of frequency in the steepest-descent plane. In Fig. 6, such a plot is obtained by

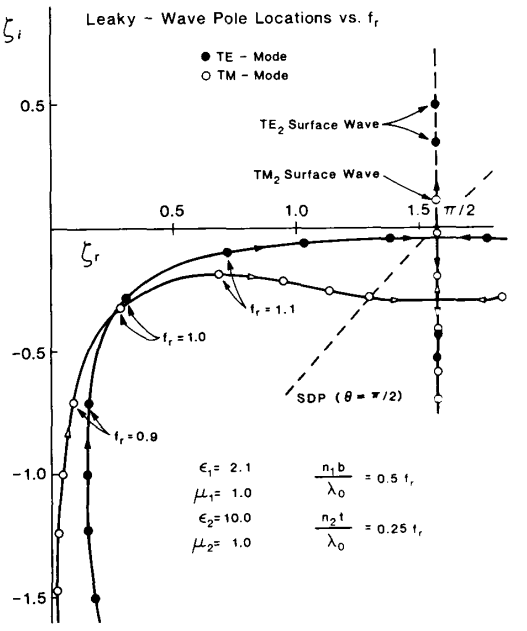

Fig. 6. Migration of leaky-wave poles in steepest-descent plane with normalized frequency f_r, for lowest mode with $\epsilon_2 = 10$. Interval between data points is 0.10.

introducing a frequency ratio f_r, and then using layer thicknesses according to

$$\frac{n_1 b}{\lambda_0} = 0.5 f_r \quad (22a)$$

$$\frac{n_2 t}{\lambda_0} = 0.25 f_r \quad (22b)$$

with $\epsilon_1 = 2.1$, $\epsilon_2 = 10$, and $\mu_1 = \mu_2 = 1$.

At low frequency the radiated beam has a maximum at broadside with a relatively low gain. For low frequency both the TE- and TM-mode poles lie significantly below the real axis, as seen in Fig. 6. As f_r increases toward 1.0 the broadside beam narrows, with a maximum broadside gain obtained for $f_r \simeq 1.0$. At this point conditions (22a) and (22b) then correspond to the resonance condition for $\theta_p = 0$ for the lowest mode ($m = 1$, $p = 1$) as given by (1) and (2). In the steepest-descent plane both poles are seen to come near to the origin at $f_r = 1$. At this point $-\zeta_i \simeq \zeta_r$, in accordance with the prediction, made in association with (17c) and (18c), that for large ϵ_2 the poles would lie near to the origin along the diagonal line.

As f_r increases past 1.0 the beam scans, since (1) is then satisfied for larger values of θ_p; (2) will then not be satisfied exactly, but this feature is not too significant in determining the resonance condition. It is primarily the substrate thickness that determines the beam scan angle. The scanned beam is conical in shape, having a narrower beamwidth in the H-plane than in the E-plane. These results are in agreement with the pole behavior for $f_r > 1.0$ in Fig. 6. As f_r increases, ζ_r increases for both poles. However, $|\zeta_i|$ decreases steadily

for the TE-mode pole but begins increasing for the TM-mode pole. The attenuation constant α is thus smaller for the TE-mode pole, in accordance with (17b), (18b) which predict that the TE-mode pole is less attenuated when $\epsilon_2 \gg 1$.

Also shown in Fig. 6 is a portion of the steepest descent path (dashed line) for the case of a saddle point at $\zeta = \theta = \pi/2$, with the path described by $\sin \zeta_r \cosh \zeta_i = 1$. All leaky-wave poles to the left of this line will be captured for some angle θ, while those to the right are never captured. This path also serves as a dividing line between fast waves ($\beta < k_0$) to the left and slow waves ($\beta > k_0$) to the right, seen from (11). Hence all leaky-waves poles which are captured, and thus directly contribute to the fields, are fast waves. From Fig. 6 it is seen that both the TE-mode and TM-mode poles cross the $\pi/2$ steepest-descent curve, but at different frequencies. The poles continue to proceed into the slow wave region, intersecting the line $\zeta_r = \pi/2$. In the lossless case, poles in the ζ-plane are symmetrically located about the line $\zeta_r = \pi/2$ [2]. Hence, at the intersection frequencies the poles merge with their symmetrical counterparts, which are also improper poles. As f_r increases further, the pole pairs split. For each pair, one pole proceeds downward along the line $\zeta_r = \pi/2$, and represents an improper surface wave pole, which is never captured for any angle θ. The other pole moves upward from the intersection point along the line $\zeta_r = \pi/2$, starting as an improper surface-wave pole. This pole crosses the $\zeta = \pi/2$ point (real axis) at the frequency corresponding to a TE or TM surface-wave cutoff frequency, for the respective pole type. The pole continues to move upward as f_r increases, becoming a proper surface-wave pole. The two upward-moving poles may then be identified as the usual TE_2 and TM_2 surface-wave poles, respectively (for the indexing used here, the TM_0 and TE_1 modes have the lowest cutoff frequencies of their respective mode types, with the TM_0 mode having zero cutoff frequency).

Although only the TE_2 and TM_2 poles are shown in Fig. 6, there are an infinite number of both TE- and TM-mode leaky-wave poles [6], although only a finite number are captured by the steepest-descent path (and hence contribute directly to the field) at any given frequency. Only the TE_2 and TM_2 poles are dominant, however, with the others being further away from the real axis. All of the leaky waves exhibit a similar behavior regarding the intersection with a symmetrical image pole on the $\pi/2$ line, however, with the upward-moving pole crossing the $\pi/2$ point at some frequency, corresponding to a surface-wave cutoff frequency. In this way all leaky-wave poles may be indexed according to their corresponding surface wave type and number.

VI. Conclusion

The narrow-beam resonance gain phenomenon discussed in [1] is shown to be attributable to the excitation of weakly attenuated leaky waves on the structure. Both a TE- and a TM-mode leaky wave become dominant for $\epsilon_2 \gg 1$, where subscript 2 refers to the superstrate. The attenuation constant α of the leaky waves tends to zero as ϵ_2 increases, behaving as $O(1/\epsilon_2)$ for a scanned beam ($\theta_p > 0$), and as $O(1/\sqrt{\epsilon_2})$ for a broadside beam ($\theta_p = 0$). The phase constant β of the leaky waves tends to $k_0 \sin \theta_p$ for $\theta_p > 0$ and tends to zero asymptotically in the same form as α when $\theta_p = 0$. Asymptotic formulas for the explicit behavior have been presented. One practical application of these formulas is a simple rule for determining how large the structure radius r_s needs to be to realize the narrow beam: $\alpha r_s \gg 1$.

The TE-mode leaky wave determines the H-plane pattern, while the TM-mode leaky wave determines the E-plane pattern. In the H-plane, the pattern due to the leaky wave by itself may be computed from Huygen's principle, and the results show excellent agreement with the total radiation pattern, furnishing additional proof that the fields at the upper interface are indeed dominated by the leaky waves. The leaky-wave approach discussed in this paper provides both significant insight into the physical processes involved in the narrow-beam resonance gain phenomenon, and methods to derive the relevant expressions in much simpler ways.

References

[1] D. R. Jackson and N. G. Alexopoulos, "Gain enhancement methods for printed circuit antennas," *IEEE Trans. Antennas Propagat.*, vol. AP-33, pp. 976-987, Sept. 1985.

[2] T. Tamir and A. A. Oliner, "Guided complex waves: Part 1, Fields at an interface," *Proc. Inst. Elec. Eng.*, vol. 110, pp. 310-324, Feb. 1963.

[3] ——, "Guided complex waves: Part 2, Relation to radiation patterns," *Proc. Inst. Elec. Eng.*, vol. 110, pp. 325-334, Feb. 1963.

[4] ——, "The influence of complex waves on the radiation field of a slot-excited plasma layer," *IRE Trans. Antennas Propagat.*, vol. AP-10, pp. 55-65, Jan. 1962.

[5] S. Barone, "Leaky wave contributions to the field of a line source above a dielectric slab," Microwave Res. Inst., Polytechnic Inst. Brooklyn, Rep. R-532-56, PIB-462, Nov. 1956.

[6] S. Barone and A. Hessel, "Part II—Leaky wave contributions to the field of a line source above a dielectric slab," Microwave Res. Inst., Polytechnic Inst. Brooklyn, R-698-58, PIB-626, Dec. 1958.

[7] L. B. Felsen and N. Marcuvitz, *Radiation and Scattering of Waves*. Englewood Cliffs, NJ: Prentice-Hall, 1973.

[8] A. Sommerfeld, *Partial Differential Equations*. New York: Academic, 1962.

[9] N. G. Alexopoulos and D. R. Jackson, "Fundamental superstrate effects on printed circuit antennas," *IEEE Trans. Antennas Propagat.*, vol. AP-32, pp. 807-816, Aug. 1984.

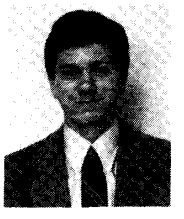

David R. Jackson (S'83-M'84) was born in St. Louis, MO, on March 28, 1957. He obtained the B.S.E.E. and M.S.E.E. degrees from the University of Missouri, Columbia, in 1979 and 1981, respectively, and the Ph.D. degree in electrical engineering from the University of California, Los Angeles, in 1985.

He is currently an Assistant Professor in the Electrical Engineering Department at the University of Houston, Houston, TX. His research interests at present include microstrip antennas and printed antennas for millimeter wave applications.

Arthur A. Oliner (M'47-SM'52-F'61-LF'87) for a photograph and biography please see page 1294 of the December 1985 issue of this TRANSACTIONS.